

1 **How woodcocks produce the most brilliant white plumage patches among the birds**

2

3 \*Jamie Dunning<sup>1</sup>, Anvay Patil<sup>2,7</sup>, Liliana D'Alba<sup>3,6</sup>, Alexander L Bond<sup>4</sup>, Gerben Debruyn<sup>3</sup>, Ali  
4 Dhinojwala<sup>3</sup>, Matthew Shawkey<sup>3</sup>, Lukas Jenni<sup>5</sup>

5

6 <sup>1</sup>Department of Life Sciences, Imperial College London, London, United Kingdom

7 <sup>2</sup>School of Polymer Science and Polymer Engineering, The University of Akron, Akron, Ohio,  
8 USA

9 <sup>3</sup>Department of Biology, Evolution and Optics of Nanostructure Group, University of Ghent,  
10 Belgium

11 <sup>4</sup>Bird Group, The Natural History Museum, Tring, United Kingdom

12 <sup>5</sup>Swiss Ornithological Institute, Sempach, Switzerland

13 <sup>6</sup>Naturalis Biodiversity Center, Leiden, the Netherlands

14 <sup>7</sup>CertainTeed LLC, Malvern, Pennsylvania, USA

15 \*Correspondence: [jamiedunning8@googlemail.com](mailto:jamiedunning8@googlemail.com); @JamieDunning

16

17 

---

Keywords: electron microscopy, reflectance, spectrophotometry, visual communication,

18 FDTD modelling

19 **Abstract**

20

21 Until recently, and when compared with diurnal birds that use contrasting plumage  
22 patches and complex feather structures to convey visual information, communication in  
23 nocturnal species was considered to follow acoustic and chemical channels. However, many  
24 nocturnal birds have evolved intensely white plumage patches within otherwise  
25 inconspicuous plumages. We used spectrophotometry, electron microscopy, and optical  
26 modelling to explain the mechanisms producing bright white tail feather tips of the  
27 Eurasian woodcock *Scolopax rusticola*. Their diffuse reflectance was ~30% higher than any  
28 previously measured feather. This intense reflectance is the result of incoherent light  
29 scattering from a disordered nanostructure composed of keratin and air within the barb  
30 rami. In addition, the flattening, thickening, and arrangement of those barbs creates a  
31 Venetian-blind-like macrostructure that enhances the surface area for light reflection. We  
32 suggest that the woodcocks have evolved these bright white feather patches for long-range  
33 visual communication in dimly lit environments.

34

35 Keywords: electron microscopy, reflectance, *Scolopax*, spectrophotometry, visual  
36 communication, FDTD modelling

## 37 1. Introduction

38

39 The use of contrasting plumage patches or complex feather structures to convey  
40 information is widespread in birds (reviewed in Jenni and Winkler 2020; Terrill and Shultz  
41 2022). Unlike in diurnal birds, visual signals in nocturnal species are understudied, and  
42 communication was, until recently, considered to follow chemical and acoustic channels  
43 (Healy and Guilford 1990; Bonadonna and Bretagnolle 2002; Grieves et al. 2022). However,  
44 in dim light environments, plumage characteristics have emerged that maximize  
45 reflectance of available light (Endler 1993; Penteriani and Del Mar Delgado 2017). While  
46 most nocturnal birds have inconspicuous or cryptic plumages, visual signals are typically  
47 intensely white; for example, the white patches in the plumage of some nightjars  
48 Caprimulgidae (Aragonés, Arias De Reyna, and Recuerda 1999), true owls Strigidae  
49 (Penteriani et al. 2007; Bortolotti, Stoffel, and Galván 2011; Bettega et al. 2013), stone-  
50 curlews Burhinidae (Cramp and Simmons 1983), and snipes Scolopacidae (Höglund,  
51 Eriksson, and Lindell 1990).

52 The function and the mechanism by which these white patches optimise light reflectance is  
53 not well understood (but see Igic, D'Alba and Shawkey 2016; Igic, D'Alba and Shawkey  
54 2018), but they communicate behavioural intention, for example, mating or territorial  
55 behaviours, or signal quality (Höglund, Eriksson, and Lindell 1990; but also see Sæther et  
56 al. 2000). However nocturnal birds typically also require crypsis while roosting during day  
57 light (Troscianko et al. 2016; Stevens et al. 2017) and therefore conceal their visual signals.  
58 White wing patches of some nightjars are, for example, only exposed in flight (Aragonés,  
59 Arias De Reyna, and Recuerda 1999), or, in the woodcocks *Scolopax* spp, white undertail  
60 feather patches are only exposed when the tail is raised (Borodulina and Formosow 1967;  
61 Figure 2.Ca - b).

62 Borodulina and Formosow (1967) first described modifications to the rami that radiate  
63 from the central rachis of the feather) that comprise the white tips on the underside of the  
64 Eurasian woodcock's *Scolopax rusticola* (hereafter woodcock) tail feathers (hereafter  
65 rectrices) but did not measure reflectance and characterise its mechanism. Previous

66 studies have demonstrated how micro-structures correlate with white plumage intensity,  
67 for example in the winter body plumage of the rock ptarmigan *Lagopus muta* (Dyck 1979),  
68 the opal-like colours on some manakin birds Pipridae (Igic, D'Alba, and Shawkey, 2016)  
69 and between many white-plumaged birds from different families (Igic, D'Alba, and  
70 Shawkey, 2018). Likewise, 'super-white', derived of micro-structures on the carapace of a  
71 beetle (Vukusic et al., 2007; Burrese et al., 2014) were well reported. The white patches in  
72 nocturnal birds, which are potentially optimised for signalling in low-light conditions, have  
73 seldom been addressed and require more detailed analysis.

74 Here we describe the mechanisms by which the white rectrix tips of the woodcock produce  
75 an intense white signal in low light conditions, using angle-resolved and diffuse  
76 spectrophotometry, electron microscopy and optical modelling via finite-difference time-  
77 domain (FDTD) approaches.

78

## 79 **2. Material and Methods**

80

### 81 **(a) Microscopy**

82 To characterize the microstructure and nanostructure responsible for producing the bright  
83 white signal, we used scanning and transmission electron microscopy (SEM and TEM,  
84 respectively). For SEM, we mounted individual white and brown rami (obtained from the  
85 same feather) separately, on stubs with carbon tape. We also oriented small fragments of  
86 rami in a way that allowed their observation in cross section. We sputter-coated the  
87 samples with gold/palladium for 2 minutes and imaged them on a SEM (FlexSEM 1000;  
88 Hitachi) at an accelerating voltage of 10 kV and 6 mm working distance.

89 For TEM we first embedded individual rami following a standard protocol (D'Alba et al  
90 2021). Briefly, we rinsed and dehydrated the rami using ethanol three times, and then  
91 infiltrated them with increasing concentrations (15%, 50%, 70% and 100%) of epoxy resin  
92 (EMbed-812; Electron Microscopy Sciences, PA, USA) followed by 16-hour polymerization  
93 in epoxy resin at 60° C in a laboratory oven.

94 We trimmed the blocks containing the rami and cut 100 nm thick cross sections using a  
95 Leica UC-6 ultramicrotome (Leica Microsystems, Germany). We collected the sections using  
96 oval-slit carbon and formvar-coated copper grids in duplicate and stained with  
97 Uranylless/lead citrate. We observed the sections on a JEOL JEM 1010 (Jeol Ltd, Tokyo,  
98 Japan) transmission electron microscope operating at 120 kV.

99

## 100 **(b) Spectrophotometry**

101 We used micro- and (macro)spectrophotometry to measure light reflectance from three  
102 separate rectrices. We measured reflectance from the reverse surface of a white ramus  
103 using a micro-spectrophotometer (CRAIC AX10; sensitivity 320-800 nm); and a  
104 spectrophotometer that measured a region across several rami (~2 mm spot size). We  
105 measured diffuse (all reflected light) and specular reflectance (light reflected at a specific  
106 angle) between 300 - 700 nm in increments of 1 nm using a AvaSpec-2048 spectrometer  
107 and dual light source set-up (AvaLight-DH-S deuterium-halogen light source and AvaLight-  
108 HAL-S-MINI light source). We measured diffuse reflectance (which assumes that light  
109 reflectance is influenced by internal structures as well as those on an object's surface)  
110 using a bifurcated probe and an integrating sphere with a black gloss trap to exclude  
111 specular (light reflected from an objects surface) reflectance (AvaSphere-50-REFL). Then,  
112 we measured specular reflectance at three different angles (75°, 60°, 45°) using a  
113 bifurcated probe and a block holder (AFH-15, Avantes). We placed each feather on black  
114 paper minimizing background reflectance. All measurements are expressed relative to an  
115 99% white reflectance standard (WS-2, Avantes) and 2% Avantes black standard (BS-2,  
116 Avantes). We processed data in the R package pavo in R 4.1.2 (Maia et al. 2019; R Core  
117 Team 2022) and plotted them with previously published measurements from 61 other  
118 birds using identical spectrophotometric methods (Igic, D'Alba and Shawkey 2018).

119

## 120 **(c) Finite-Difference Time-Domain (FDTD) simulations**

121 To explore the directionality of reflectance as a function of varying rami angle, we modelled  
122 how photons interact with structures within an individual barb. We ran a series of finite-  
123 difference time-domain (FDTD) simulations using a commercial-grade Ansys Lumerical  
124 2021 R1 solver (Ansys, Inc.). The FDTD method provides a general solution to any light  
125 scattering problem on complex arbitrary geometries (in this case, a unit cell structure of an  
126 individual ramus) by numerically solving Maxwell's curl equations on a discrete  
127 spatiotemporal grid (Taflove and Hagness 2005). The simulation estimates all scattered  
128 light at all angles and, in this respect, is not directly comparable with our diffuse  
129 spectrophotometry data.

130 Our simulated 3D CAD models were based on empirical microscopic observations of the  
131 woodcock barbs (see supplementary material, S1:A-D). First, we rendered a 3D CAD  
132 geometry for a control hollow unit cell, without internal photonic nanostructures, and a  
133 solid unit cell. We used SEM microscopy to define CAD dimensions, each cell had a keratin  
134 cortex thickness of 7  $\mu\text{m}$  with a hollow interior, 20  $\mu\text{m}$  high (Z direction) and 8  $\mu\text{m}$  wide (X  
135 direction). We then used SEM microscopy to render a unit cell with an internal  
136 nanostructure equivalent to the woodcock's rami, i.e. of air pockets and a supporting  
137 matrix of nano-fibres (see Figure 1). We did this using a uniform random distribution of  
138 non-overlapping spherical particles within the keratin matrix, which randomly varied in  
139 diameter between 0.45  $\mu\text{m}$  and 3.45  $\mu\text{m}$ . The optical constants (complex refractive indices)  
140 for keratin were adapted from previous literature (Stavenga et al. 2015; Table S1).

141 We performed simulations using a broadband plane wave source (400-700 nm),  
142 propagated along the -Z direction. First, at a normal angle of incidence (AOI;  $0^\circ$  from cell  
143 surface) and then at  $70^\circ$ , for our control, hollow and solid, unit cells. Then, we ran  
144 simulations using our simulated woodcock cell at  $0^\circ$ ,  $20^\circ$ ,  $50^\circ$ ,  $70^\circ$  and  $80^\circ$  AOI. Boundary  
145 conditions in the lateral direction (X and Y) were set to periodic. We monitored reflectance  
146 data using a Discrete Fourier Transform (DFT) power monitor placed behind the source  
147 injection plane. The simulation time (in fs) and boundary condition along the light  
148 propagation direction (Z; perfectly matching layer (PML) boundaries) were chosen such

149 that the electric field decayed before the end of the simulation (auto-shutoff criteria). All  
150 the incident light was either reflected, transmitted, or absorbed.

151

### 152 **3. Results**

#### 153 **(a) Structure of the white rectrix tips**

154 The tips of the rectrices are white on the reverse (figures 1A and 2A), but greyish brown on  
155 the obverse surface (figure 1B). The rami are thickened and flattened in the white patch  
156 and overlap each other, superficially like Venetian-blinds (figures 1C, 1E). The angle of  
157 these rami relative to the feather surface vary (as suggested by Borodulina and Formosow  
158 1967), we estimated from  $\sim 70^\circ$  for proximal rami to  $\sim 76^\circ$  for distal rami (figure 1E). The  
159 proximal and distal brown barbules originate from the upper surface of the rami, hence are  
160 only visible on the obverse surface and cover the thickened white rami from above,  
161 providing the greyish brown colour of the obverse surface (figures 1B and 1D). They  
162 interlock to form a coherent vane. The two sides of a white tip, separated by the rachis, are  
163 concave and the barbs arranged in opposite angles (figure 1J), reflecting light in different  
164 directions and apparent when turning a feather in low light. In contrast, the brown parts of  
165 the rectrices are structurally typical of vaned feathers with thin barbs that are spaced by  
166 the brown barbules (figure 1J, 1K). The thickened white rami in the feather tips were  $\sim 2.5$   
167 times thicker and appeared internally more complex than brown rami (figure 1 F-H and 1J-  
168 M, respectively). The medulla of white rami contained numerous and complex photonic  
169 cells with fine networks of nanofibers and scattered air pockets (figure 1G-I), lacking  
170 melanosomes entirely. These matrices of air and keratin appeared disorganized. In  
171 contrast, rami from brown feather regions were less thick, rounder, had fewer medullary  
172 cells and did not contain a matrix of air and keratin, but were abundant in melanosomes  
173 both inside the barb medulla and the cortex (figure 1K-M).

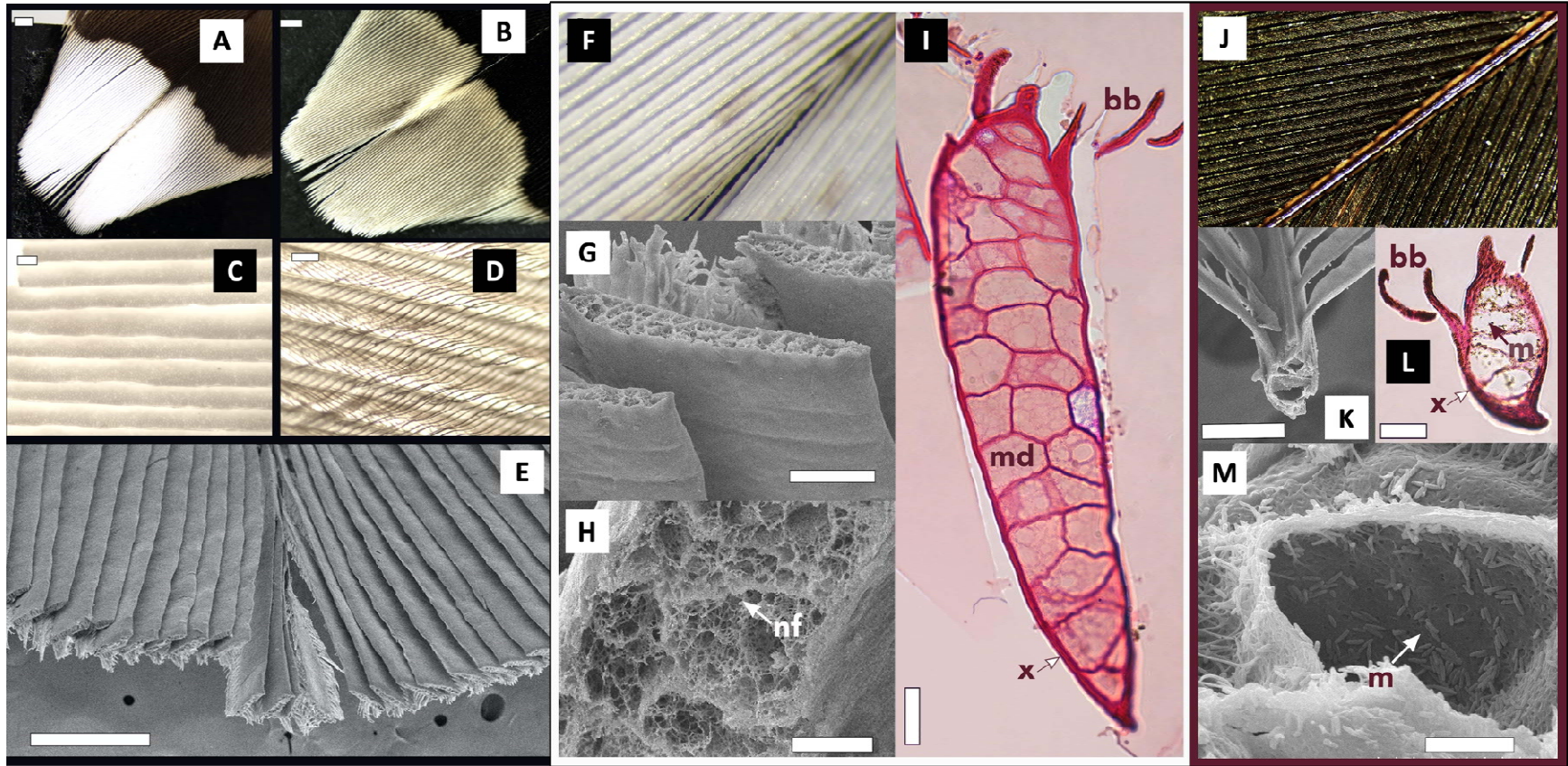
174

#### 175 **(b) Reflectivity**

176 Spectrophotometry revealed intense diffuse reflectance across rami on the white underside  
177 of the rectrices, peaking at 55% (628 nm) (figure 1F; 2A). Likewise, individual rami had

178 even greater specular reflectance, peaking >100% against a diffuse standard  
179 (supplementary figure S2). The white patches on woodcock rectrices are therefore  
180 exceptionally bright, and, to the best of our knowledge, represent the brightest white  
181 measured from the plumage of a bird, 31% brighter than the next most reflective, Caspian  
182 tern *Hydroprogne caspia*, that peaks at 38% (459nm), and 91% brighter than the least-  
183 reflective white feather measured, arctic redpoll *Acanthis hornemanni*, that peaks at 4.9%  
184 (638nm) (Igic, D'Alba, and Shawkey 2018; figure 2A). Specular reflectance was highest  
185 when measured at 75° relative to surface normal, decreasing at more acute angles,  
186 suggesting some directionality to reflectance intensity (supplementary figure S3).  
187





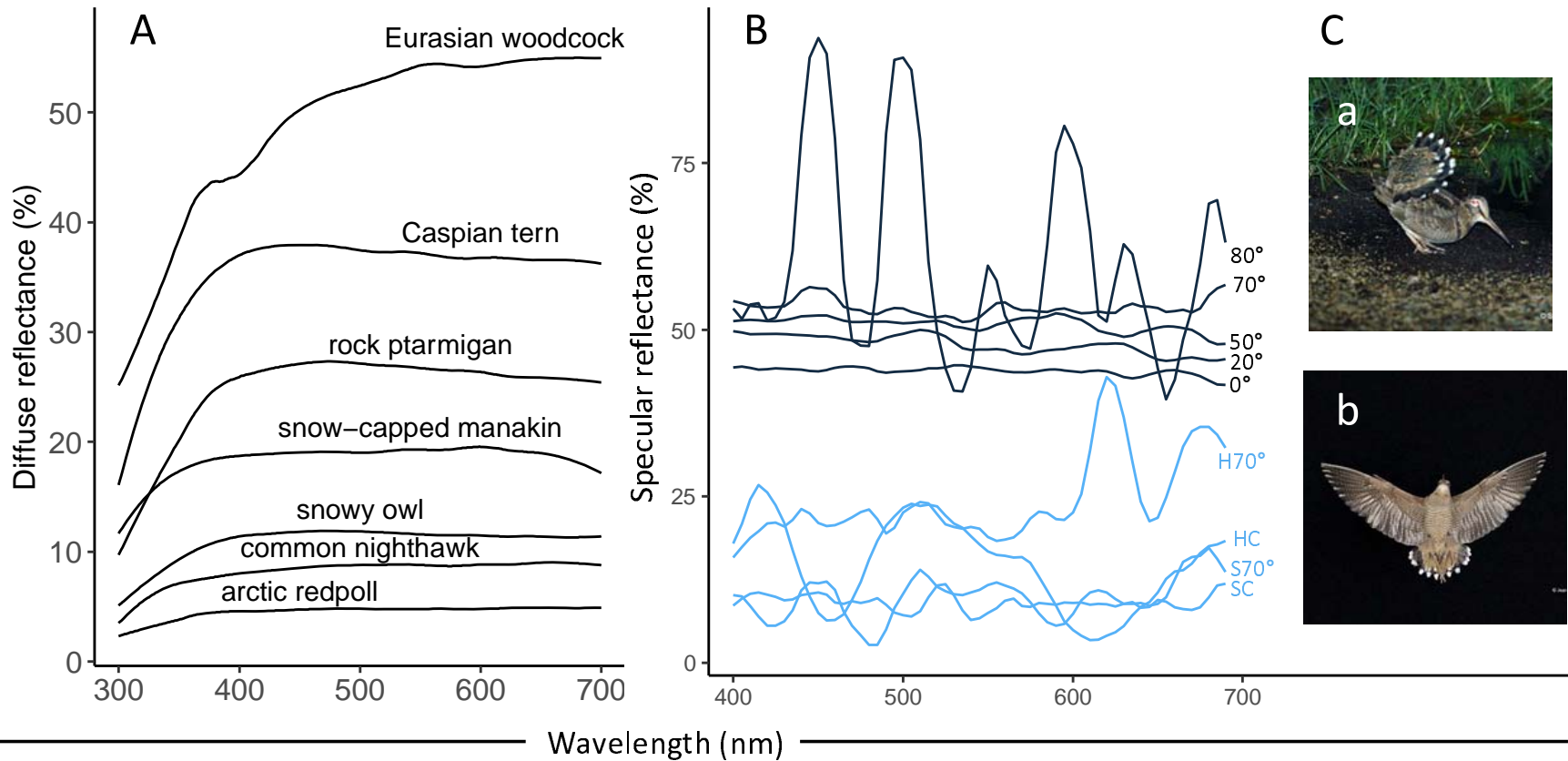
188

189 **Figure 1. A) – E): Morphology of the white tips of woodcock *Scolopax rusticola* rectrices.** A) White reverse surface. B)  
 190 Brown obverse surface. C) White rami in a Venetian-blind alignment; individual cells are apparent. D) Obverse view showing  
 191 the interlocked dark barbules covering the white rami. E) SEM micrograph of the white rectrix tip transversally cut, showing  
 192 shallow V-shaped surface of rami; **F) – M): Comparison of the microstructure of the white and brown parts of rectrices.**  
 193 F) Optical image of white rami. G) Thickened and flattened rami viewed from the reverse surface. H) Interior of a white ramus  
 194 shows cells with networks of keratin fibres (nf) and air pockets. I) a white ramus showing hollow medullary cells (md) and a

195 thin cortex (x); the barbules (bb) are present on the obverse side. J) Optical image of contiguous brown region. K) Brown rami  
196 in cross-section. L) Melanosomes (m) present throughout the rami and barbules. M) Medullary cell of brown ramus showing  
197 melanosomes (m) and the absence of keratin matrices. Scale bars: A and B) 1mm; C), D), G) and K) 50 $\mu$ m; E) 500 $\mu$ m; H) 10 $\mu$ m;  
198 I) and L) 100 $\mu$ m; M) 5 $\mu$ m.

199

200



203 Figure 2. (A) Diffuse reflectance spectra measured from the reverse surface of the white Eurasian woodcock *Scolopax rusticola*  
 204 rectrix tips, peaking at ~55%, 31% brighter than the next brightest feather, Caspian tern *Hydroprogne caspia*, and compared  
 205 against 61 white plumages from Igc, D'Alba, and Shawkey (2018), species mentioned in text are highlighted; (B) Finite-  
 206 Difference Time-Domain (FDTD) simulations showing simulated reflectance at five angles of incidence (AOI; highlighted in

207 grey, 0, 20, 50, 70 and 80) and four control measurements (highlighted in blue; hollow cell at 70 AOI, hollow cell control, solid  
208 cell at 70 AOI and solid control). These data suggest that air pockets present in the keratin matrix are essential for increasing  
209 the reflectivity across visible wavelengths in the woodcock's tail feathers. (C) Showing ecological context when white tips are  
210 exposed, either from the ground (probably a female attracting an overflying male) (Ca) or in flight (male in display flight) (Cb);  
211 photos by Serge Santiago and Jean-Lou Zimmermann,

## 212 **(c) Finite-Difference Time-Domain simulations of reflectivity**

213 We found the disordered nanostructure formed by keratin and air phases in the woodcock  
214 rami were essential for generating intense white reflectance. For normal incidence ( $0^\circ$  from  
215 the surface normal), the overall reflectance for the woodcock-mimicked rami unit cell  
216 nanostructure increased by  $\sim 65\%$  with respect to the control hollow unit cell  
217 nanostructure. Additionally, the simulations also highlight some directionality to patch  
218 intensity. Modelled reflectance at  $80^\circ$ , although showed high reflectance, also showed  
219 increased noise, which we suggest is due to interference effects on the surface of the  
220 feather structures. Otherwise, the reflectance increased from a peak of  $\sim 45\%$  at normal  
221 incidence ( $0^\circ$ ), to a peak of  $\sim 57\%$  at  $70^\circ$ , which represents the actual angle of the rami  
222 within the white patch (figure 2B). Reflectance at  $70^\circ$  is broadly the same as the actual  
223 diffuse reflectance (figure 2A), although FDTD simulates diffuse plus specular reflectance.  
224 We therefore suggest that the rami are arranged to lie at the angle which best optimizes  
225 reflectance. Further, our simulated control cells demonstrate that air pockets in the keratin  
226 matrix are essential for increasing the overall reflectivity across visible wavelengths.

227

228

## 229 **Discussion**

230 Our results suggest that the white tips on the woodcock's rectrices represent the brightest  
231 reflectance yet measured and, by virtue, the whitest white plumage patch currently known  
232 among the birds. Other bright white plumages have been reported previously, but they are  
233 either supposition (Tickell 2003), or using different methods or without standardised  
234 comparison (Dyck 1979; Caswell & Prum 2011). We present our results alongside those  
235 previously described plumages (see Igc, D'Alba, and Shawkey 2018 for a full list), using  
236 standardised a approach (Figure 2A). This reflectance is produced by the arrangement of  
237 thick and flattened rami with a broad distribution of air pockets, that together maximize  
238 light reflectance. We used FDTD simulations to demonstrate that 1) the internal structure  
239 of the rami on the white tips is integral for light scattering and subsequent reflectance, but  
240 also; 2) that the angle of the broadened barbs in relation to each other optimise reflectance  
241 at the macro-scale.

242 The structures we describe differ from those of less intense diurnal plumages in two ways:  
243 First, the rami are thickened and flattened (Borodulina and Formosow 1967; this study),  
244 increasing surface area available for reflection and preventing light from passing between  
245 the rami and barbules. Second, the thickened rami allow for a complexity of photonic cells,  
246 with a network of keratin nanofibers and scattered air pockets, creating numerous  
247 interfaces to favour scattering events (which similar to the ‘super-white’ reflectance  
248 described in a white beetle; Vukusic 2007, Burrese et al. 2014).

249 Igit, D’Alba, and Shawkey (2018) suggested that more intense reflectance of white plumage  
250 was associated with densely packed, rounder and less hollow rami, but also thicker and  
251 longer barbules. Consequently, larger species were brighter by virtue of rami thickness and  
252 complexity. However, the woodcock rami are thickened and flattened, superficially like the  
253 rami in the white crown of Blue-rumped Manakin *Lepidothrix isidorei* (Igit, D’Alba, and  
254 Shawkey 2016); in this case, the internal nanostructure is without the thickened rami that  
255 increases the surface area of reflectance. Despite some similarities, the diffuse reflectance  
256 of the manakin’s crown peaks at ~17% (Igit, D’Alba, and Shawkey 2016), ~105% less  
257 bright than the woodcock. However, specular reflectance of the manakin crown is higher  
258 than the woodcock, due to a nanostructure that enhances specular reflectance (also see  
259 Shawkey, Maia and D’Alba 2011; McCoy et al. 2021).

260 The Venetian-blind arrangement of the thickened rami, and subsequent directional  
261 reflectance, is like the arrangement of barbules of hummingbirds Trochilidae. Here, the  
262 angle of the barbules relative to the axis of the ramus, and the angle between the proximal  
263 and distal barbules of the rami determine directionality of reflectance, associated with  
264 irradiance (Giraldo, Sosa and Stavenga, 2021).

265 White patches are present in all eight species of woodcock, but not in their closest relatives  
266 (23 species of non-*Scolopax* Scolopacidae, see supplementary table S1) and signal some  
267 behavioural intention in dimly lit environments (Cramp and Simmons 1983; Glutz von  
268 Blotzheim et al., 1977). Because these patches are only visible from below, any functional  
269 significance is conditional on raising and fanning the tail, for example during courtship  
270 displays (Hagen, 1950; Hirons, 1980; Ferrand and Gossmann 2009; Lastukhin and Isakov,



271 2016), predator distraction or non-reproductive communication (Ingram, 1974; Fetisov,  
272 2017). The link between patch intensity, behaviour and relative light environment is  
273 understudied and would benefit from further research.  
274 We suggest that the woodcocks have evolved brilliant white feather patches, the brightest  
275 described within the birds, through elaborate structural modifications at the macro-,  
276 micro- and nano scales for communication in dimly lit environments.

277

278

## 279 **Acknowledgments**

280 We would like to thank Mary Hennen, Michael A Pearson, Matt Rayner, Paul Sweet, Arseny  
281 Tsvey, Niklaus Zbinden for conversation, samples, and translations, and Serge Santiago and  
282 Jean-Lou Zimmermann for the photos. AD and AP acknowledge financial support from the  
283 US Air Force Office of Scientific Research (AFOSR) under Multidisciplinary University  
284 Research Initiative (MURI) grant (FA 9550-18-1-0142).

## 285 **Ethics statement**

286 We sourced woodcock rectrices from a private collection from Switzerland without the  
287 need for specific licensing.

288

289 **References**

290

291 Aragonés, J., L. Arias De Reyna and P. Recuerda. 1999. Visual communication and sexual  
292 selection in a nocturnal bird species, *Caprimulgus ruficollis*, a balance between crypsis and  
293 conspicuousness. *Wilson Bull.* 111(3): 340-345. <https://www.jstor.org/stable/4164097>.

294 Bettega, C., L. Campioni, M. Del Mar Delgado, R. Lourenço and V. Penteriani. 2013.  
295 Brightness features of visual signalling traits in young and adult Eurasian eagle-owls. *J.*  
296 *Raptor Res.* 47(2): 197-207. doi.org/10.3356/JRR-12-00002.1.

297 Bonadonna, F. and V. Bretagnolle. 2002. Smelling home: A good solution for burrow-finding  
298 in nocturnal petrels?. *J. Exp. Biol.* 205(16): 2519–2523. doi.org/10.1242/jeb.205.16.2519.

299

300 Borodulina, T.L. and A.N. Formosow. 1967. About signal spots of feathering of birds and  
301 peculiarity of Woodcock rectrices (in Russian). *Bjull. Mosk. obstsch. ispyt. prirody, otd. biol.*  
302 72(3): 27–31. -- Also published in *Russkii Ornitologicheskii Zhurnal* 24. 2015. Ekspress  
303 Vypusk 1230: 4622-4626.

304 Bortolotti, G. R., M. J. Stoffel and I. Galván. 2011. Wintering Snowy Owls *Bubo scandiacus*  
305 integrate plumage colour, behaviour and their environment to maximize efficacy of visual  
306 displays. *Ibis.* 153(1): 134-142. doi.org/10.1111/j.1474-919X.2010.01067.x.

307 Burrese, M., L. Cortese, L. Pattelli, M. Kolle, P. Vukusic, D.S. and Wiersma, S. Vignolini. 2014.  
308 Bright-white beetle scales optimise multiple scattering of light. *Sci Rep*, 4(1): 6075.  
309 doi.org/10.1038/srep06075.

310 Stoddard, M. C., and Prum, R.O. 2011. How colorful are birds? Evolution of the avian  
311 plumage color gamut, *Beha. Ecol.* 22(5):1042–  
312 1052, <https://doi.org/10.1093/beheco/arr088>

313 Cramp, S., and K.E.L. Simmons. 1983. *Handbook of the Birds of Europe, the Middle East and*  
314 *North Africa. The Birds of the Western Palearctic, Vol. 3.* Oxford University Press, Oxford.

315

316 D'Alba, L., M. Meadows, R. Maia, Y. Jong-Souk, M. Manceau, and M. Shawkey. 2021.  
317 Morphogenesis of iridescent feathers in Anna's hummingbird *Calypte anna*. *Integrative and*  
318 *Comparative Biology.* icab123, doi.org/10.1093/icb/icab123

319

320 Dyck, J. 1979. Winter plumage of the rock ptarmigan: structure of the air-filled barbules  
321 and function of the white colour. *Dansk. Orn. Foren. Tidsskr*, 73, pp.41-58.

322

323 Endler J.A. 1993. The color of light in forests and its implications. *Ecological monographs.*  
324 63(1): 1-27 doi/abs/10.2307/2937121.

325

326 Ferrand Y. and F. Gossmann. 2009. *La Bécasse des bois.* Effet de lisière éditeur, Saint-Lucien,  
327 France.

328



- 329 Fetisov C.A. 2017. On the functional significance of bright white spots on the tail of the  
330 woodcock *Scolopax rusticola* (in Russian). *Russkii Ornitologicheskii Zhurnal* 26, Ekspres  
331 Vypusk 1466: 2727–2733.  
332
- 333 Giraldo M., J. Sosa and D. Stavenga. 2021. Feather iridescence of *Coeligena* hummingbird  
334 species varies due to differently organized rami and barbules. *Biol Lett*, 17(8): 20210190.  
335 [doi.org/10.1098/rsbl.2021.0190](https://doi.org/10.1098/rsbl.2021.0190).
- 336  
337 Glutz Von Blotzheim, U. N., K. M. Bauer and E. Bezzel. 1977. *Handbuch der Vögel*  
338 *Mitteleuropas* Vol 7. Akademische Verlagsgesellschaft, Leipzig.
- 339 Grieves L.A., M. Gilles, I.C. Cuthill, T. Székely, E.A. MacDougall-Shackleton and B.A. Caspers.  
340 2022. Olfactory camouflage and communication in birds. *Biol Rev.* 97(3): 1193-  
341 1209. [doi.org/10.1111/brv.12837](https://doi.org/10.1111/brv.12837).  
342
- 343 Hagen, Y. 1950. How a Woodcock (*Scolopax rusticola*) sitting on the ground attracts the  
344 attention of partners in mating flight. *Vår Fågelvärld* 9:195–199.  
345
- 346 Healy, S. and T. Guilford. 1990. Olfactory-bulb size and nocturnality in birds. *Evolution*,  
347 44(2): 339–346. [doi.10.1111/j.1558-5646.1990.tb05203.x](https://doi.org/10.1111/j.1558-5646.1990.tb05203.x)  
348
- 349 Hirons, G., 1980. The significance of roding by Woodcock *Scolopax rusticola*: an alternative  
350 explanation based on observations of marked birds. *Ibis* 122, 350–354. [doi.10.1111/j.1474-](https://doi.org/10.1111/j.1474-919X.1980.tb00888.x)  
351 [919X.1980.tb00888.x](https://doi.org/10.1111/j.1474-919X.1980.tb00888.x).  
352
- 353 Höglund, J., M. Eriksson and L. E. Lindell. 1990. Females of the lek-breeding great snipe,  
354 *Gallinago media*, prefer males with white tails. *Anim. Behav.* 40(1): 23-32.  
355 [doi.org/10.1016/S0003-3472\(05\)80662-1](https://doi.org/10.1016/S0003-3472(05)80662-1).
- 356  
357 Igic, B., L. D'Alba and M. D. Shawkey. 2016. Manakins can produce iridescent and bright  
358 feather colours without melanosomes. *J. Exp. Biol.* 219 (12): 1851–9.  
359 <https://doi.org/10.1242/jeb.137182>.
- 360 Igic, B., L. D'Alba and M. D. Shawkey. 2018. Fifty shades of white: how white feather  
361 brightness differs among species. *Sci. Nat.* 105(18): 3-4. [doi.org/10.1007/s00114-018-](https://doi.org/10.1007/s00114-018-1543-3)  
362 [1543-3](https://doi.org/10.1007/s00114-018-1543-3).
- 363 Ingram, C. 1974. Possible functions of the tail spots in the Woodcock. *Brit. Birds.* 67: 475–  
364 476.  
365
- 366 Jenni, L. and R. Winkler. 2020. *The Biology of Moult in Birds*. London: Helm.

- 367 Lastukhin, A.A. and A.M Isakov. 2016. Reflection of light from white spots on the tail of a  
368 woodcock *Scolopax rusticola* in flight (in Russian). *Russkii Ornitologicheskii Zhurnal* 25,  
369 *Ekspress Vypusk*. 1312: 2642–2643.  
370
- 371 Maia R., H. Gruson, J.A. Endler, and T.E. White. 2019. pavo 2: New tools for the spectral and  
372 spatial analysis of colour in R. *Methods Ecol Evol*, 10(7):1097–1107.  
373 [Doi.org/10.1111/2041-210x.13174](https://doi.org/10.1111/2041-210x.13174).
- 374 McCoy, D.E., Shultz, A.J., Vidoudez, C., van der Heide, E., Dall, J.E., Trauger, S.A. and Haig, D.  
375 2021. Microstructures amplify carotenoid plumage signals in tanagers. *Sci Rep*, 11(1), pp.1-  
376 20.
- 377 Penteriani, V., and M. Del Mar Delgado. 2017. Living in the dark does not mean a blind life:  
378 Bird and mammal visual communication in dim light. *Proc R Soc B*. 372(1717):20160064.  
379 [doi.org/10.1098/rstb.2016.0064](https://doi.org/10.1098/rstb.2016.0064).
- 380 Penteriani, V, M. Del Mar Delgado, C. Alonso-Alvarez, and F. Sergio. 2007. The importance of  
381 visual cues for nocturnal species: Eagle owls signal by badge brightness. *Behav. Ecol*.  
382 18(1):143-147. <https://doi.org/10.1093/beheco/arl060>.
- 383 R Core Team. 2022. R: A Language and Environment for Statistical Computing. Vienna,  
384 Austria: R Foundation for Statistical Computing. Retrieved from <http://www.R-project.org/>  
385 Sæther, S. A., P. Fiske, J. A. Kålås, and J. M. Gjøl. 2000. Females of the lekking great snipe do  
386 not prefer males with whiter tails. *Anim. Behav.* 59 (2): 273–280.  
387 [doi.org/10.1006/anbe.1999.1301](https://doi.org/10.1006/anbe.1999.1301).
- 388 Shawkey, M.D., Maia, R. and D'Alba, L. 2011. Proximate bases of silver color in anhinga  
389 (*Anhinga anhinga*) feathers. *J. Morphol*, 272(11), pp.1399-1407.  
390
- 391 Stavenga, D.G., H. L. Leertouwer, D. C. Osorio and B. D. Wilts. 2015. High refractive index of  
392 melanin in shiny occipital feathers of a bird of paradise. *Light Sci. Appl.* 4:e243.  
393
- 394 Stevens, M., J. Troscianko, J. K. Wilson-Aggarwal and C. N. Spottiswoode. 2017.  
395 Improvement of individual camouflage through background choice in ground-nesting birds.  
396 *Nat. Ecol. Evol.* 1:1325-1333. [doi.org/10.1038/s41559-017-0256-x](https://doi.org/10.1038/s41559-017-0256-x).
- 397 Taflove, A. and S. C. Hagness. 2005. *Computational Electrodynamics – The Finite-Difference*  
398 *Time-Domain Method*, 3<sup>rd</sup> ed. Artech House, Inc., Norwood, MA.
- 399 Terril, R. S. and Shultz, A.J. 2022. Feather function and the evolution of birds. *Biol Rev.*  
400 <https://doi.org/10.1111/brv.12918>
- 401 Tickell, W. L. N. 2003. White Plumage. *Waterbirds: The International Journal of Waterbird*  
402 *Biology*, 26(1), 1–12. <http://www.jstor.org/stable/1522461>  
403 Troscianko, J., J.K. Wilson-Aggarwal, M. Stevens and C. N. Spottiswoode. 2016. Camouflage  
404 predicts survival in ground-nesting birds. *Sci. Rep.* 6:19966. [doi.org/10.1038/srep19966](https://doi.org/10.1038/srep19966).

405 Vukusic, P., B. Hallam and J. Noyes. Brilliant whiteness in ultrathin beetle scales. 2017.  
406 *Science*. 315:348. doi.10.1126/science.1134666.